Higher-order clustering statistics

in the Intergalactic Medium using Lyman-α forest

Soumak Maitra

IUCAA, Pune, India

Collaborators: Prof. Raghunathan Srianand (Guide), Prof. Patrick Petitjean, Prof. Tirthankar Roy Choudhury, Dr. Prakash Gaikwad, Prof. Nishikanta Khandai, Prof. Aseem Paranjape, Prof. Christophe Pichon, Dr. Hadi Rahmani

Lyman-α forest

- Majority of the baryonic content of the Universe lies in the Intergalactic Medium (IGM).
- Tracer of large scale cosmic density fields.
- Probes the astrophysical processes associated with galaxies and the circumgalactic medium (CGM) at small scales.
- Baryonic pressure broadening retains memory of the thermal history of Universe.

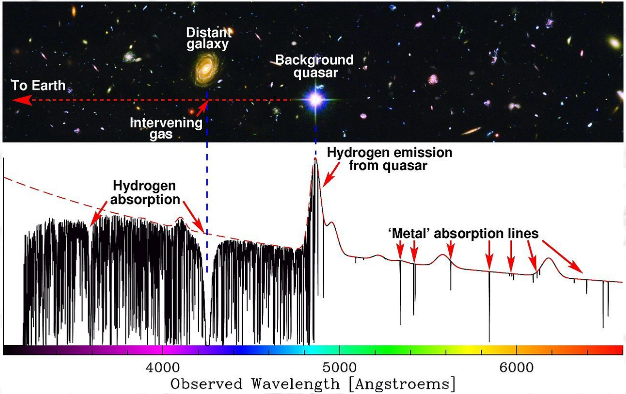

- Matter distribution in the IGM manifests itself in the form of HI Lyman-α forest absorption in the spectra of distant quasars.
- Lyman-α forest probes matter in a quasi-linear regime (experiences the gravitational potential but not a virialized system).

Ionization state of the IGM: Fluctuating Gunn-Peterson optical depth

- $F_{obs} = F_{cont}\, e^{-\tau_{\mathrm{HI}}}$
- $\tau_{\mathrm{HI}} = \int dl\, n_{\mathrm{HI}}\, \sigma_{\mathrm{HI}} \;\sim\; 10^5\, X_{\mathrm{HI}}$
- Non-trivial mapping from dark matter overdensity to n_{HI}. Interpretation of observed data requires simulations to implement the baryonic physics.

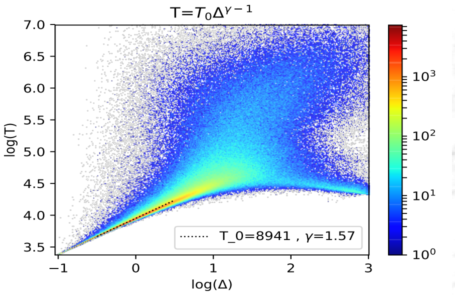

- Under the assumption of thermal and ionization equilibrium, and ignoring the effects of thermal broadening, the Gunn-Peterson optical depth is given as:

$$\tau_{\mathrm{HI,GP}} = 0.172\,\Delta^{2-0.7\gamma}\left(\frac{\Omega_b h^2}{0.0125}\right)^2\left(\frac{H(z)/H_0}{5.51}h\right)^{-1}\left(\frac{1+z}{4}\right)^6\left(\frac{\mathrm{T_0}}{10^4\mathrm{K}}\right)^{-0.7}\left(\frac{\Gamma}{10^{-12}s^{-1}}\right)^{-1}\left(1+\frac{dv_{los}/dx}{H(z)}\right)^{-1}$$

- Larger Overdensities typically correspond to larger τ_{HI}. Correlations in transmitted flux can be used as a probe of underlying overdensity field (Non-trivial mapping from density to Flux).
- Alternative approach is to construct a count-based correlation statistics using distinct absorber treatment of Lyman-α forest.

Clustering study based on cloud picture

Flux-based statistics:

- $\xi(\Delta r) =< \delta_F(r)\delta_F(r+\Delta r) >$ where $\delta_F = F - < F >$
- $\zeta(\Delta r_{12}, \Delta r_{13}, \theta) =< \delta_F^1 \delta_F^2 \delta_F^3 >$

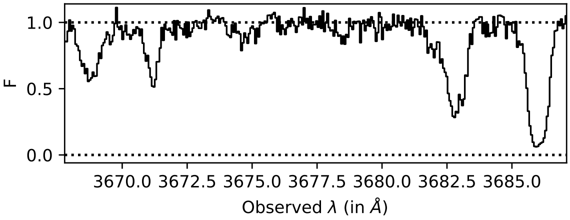

Cloud-based statistics:

- $\xi =< \frac{\textit{Data pairs}}{\textit{Random pairs}} - 1 >$
- $\zeta =< \frac{\textit{Data triplets}}{\textit{Random triplets}} - 1 >$
- Advantages:
    - Allows column density (or conversely Δ) dependent clustering study.
    - Direct probe of non-gaussianity in clustering.

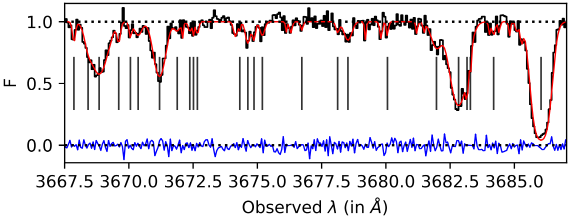

Automated Voigt profile fitting routine: VIPER (Gaikwad+2017)

Lyman-α forest: Cosmological Utility

Linear Theory Power spectrum (McDonald+2005)

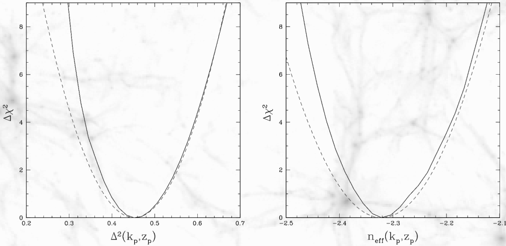

Warm Dark Matter model (Irsic+2017)

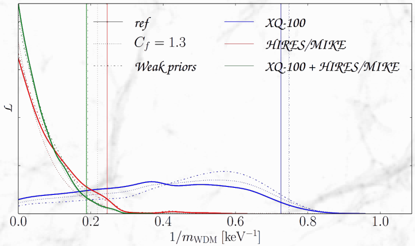

Primordial Power spectrum (Viel+2004)

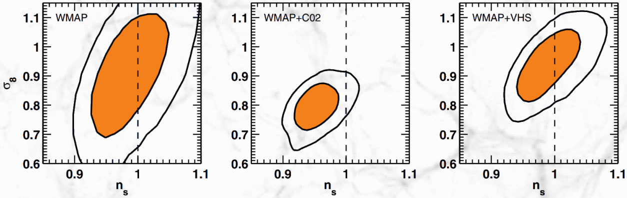

Neutrino Mass (Yeche+2017)

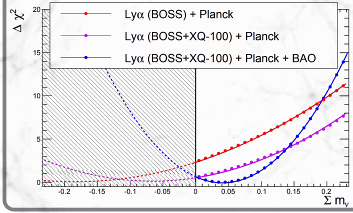

Lyman-α forest: Astrophysical Utility

IGM Thermal Evolution (Gaikwad+2020)

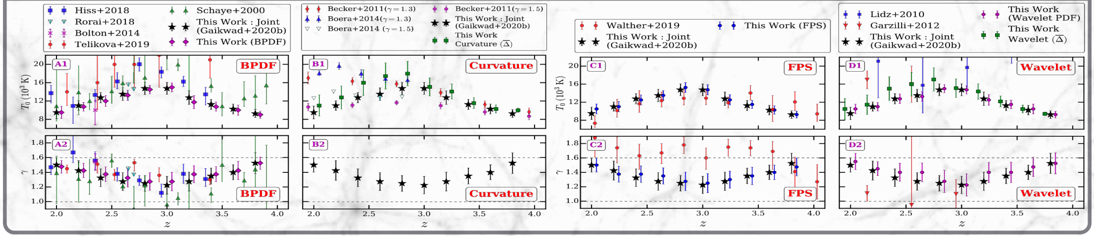

UV Background (Khaire+2019)

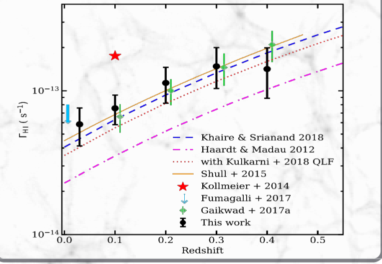

Pressure broadening scale: Sensitive to thermal history (Rorai+2017)

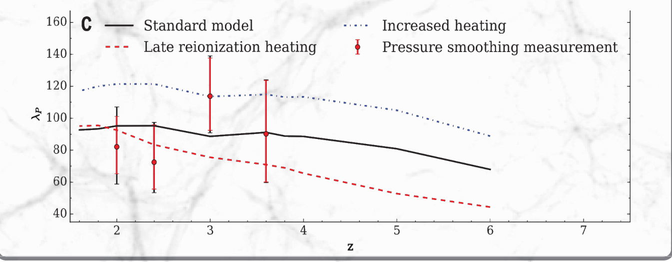

Clustering in Lyman-α forest

Redshift space (Irsic+2017)

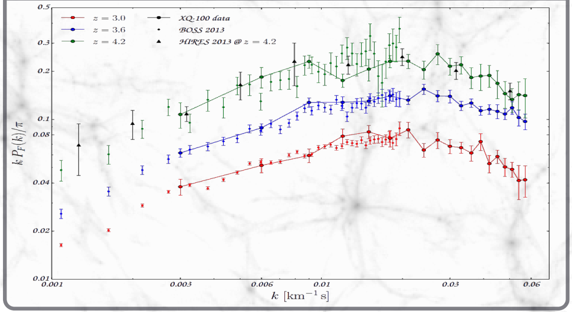

Transverse (Coppolani+2006)

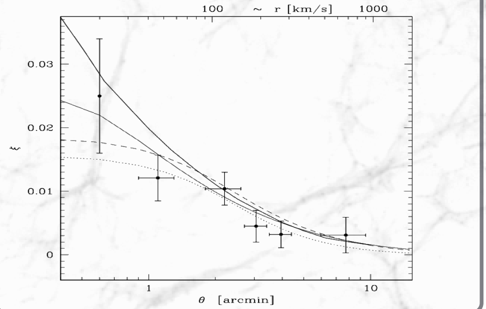

Clustering in Lyman-α forest

Redshift space (Irsic+2017)

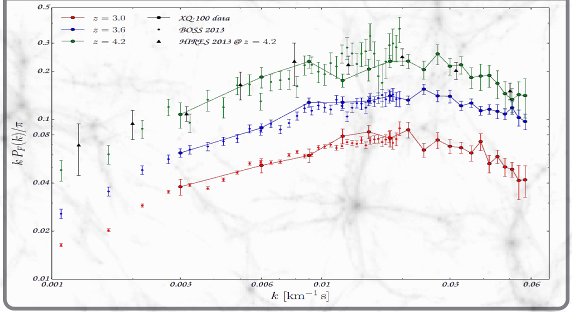

Transverse (Coppolani+2006)

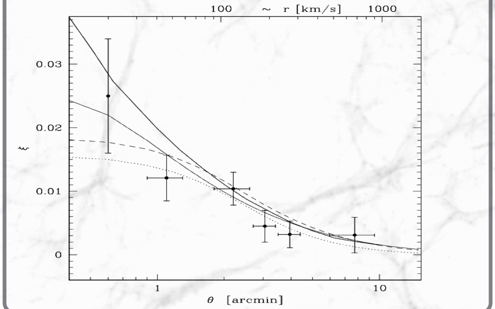

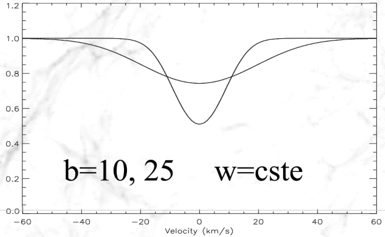

- Peeples+2010a,b demonstrate that redshift space correlations are dominated by thermal broadening ($b = \sqrt{2kT/m}$) effects while transverse correlations are dominated by pressure broadening.
- Thermal broadening washes away clustering informations at small scales.

Higher order clustering statistics in Lyman-α forest

Higher order clustering statistics largely unexplored in the case of Lyman-α forest.

Three-point statistics of clustering in Lyman-α forest would be useful for:

- Non-gaussianity in matter distribution at small scales and at high redshifts. Also calculate higher order bias.
- Act as an independent tool complementing the two-point statistics in constraining the cosmological parameters (Fry 1994, Verde+2002) and the physical state of the IGM.
- Remove degeneracies between different cosmological parameters.
- Determine the amplitude, slope and curvature of the slope of the matter power spectrum with better precision (Mandelbaum+2003).
- Probing primordial non-gaussianity (Hazra & Sarkar 2012)
- Probe the influence of large scale fluctuations on small scale power spectrum using squeezed limit bispectrum (Zaldarriaga+2001).
- Probing the statistical anisotropy of clustering in the cosmic web, using projected quasar triplet sightlines.

Redshift space correlation.

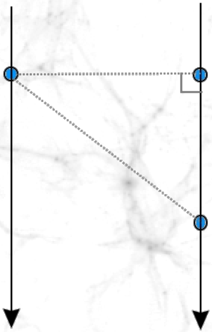

Partial Redshift space + transverse correlation.

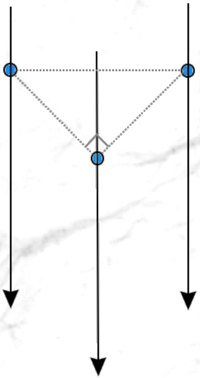

Transverse correlation.

First detection of non-gaussianity in low-z Lyman-α forest (Maitra+2020b)

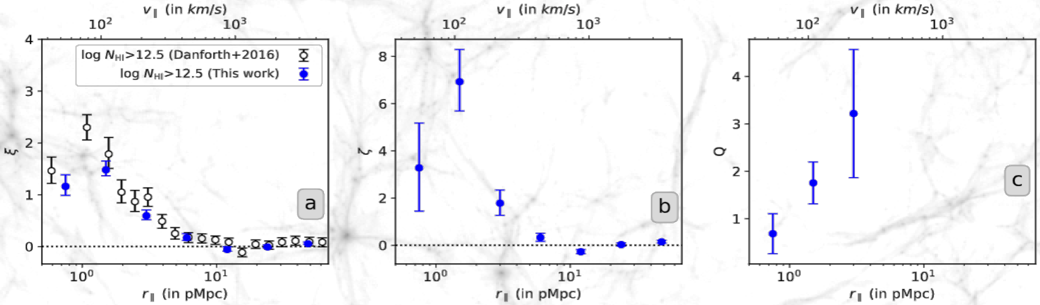

- 82 quasar sightlines from HST-COS
- Redshift based clustering study (colinear triplet configurations probed along quasar sightlines; $r_1 = r_2 = r_{||}, r_3 = 2r_{||}$).
- Lyman-α forest probed in $z < 0.48$.

Reduced ζ or Q=$\zeta/(\xi_1 \times \xi_2 + \xi_2 \times \xi_3 + \xi_3 \times \xi_1)$
[Hierarchical Ansatz]

First detection of non-gaussianity in low-z Lyman-α forest (Maitra+2020b)

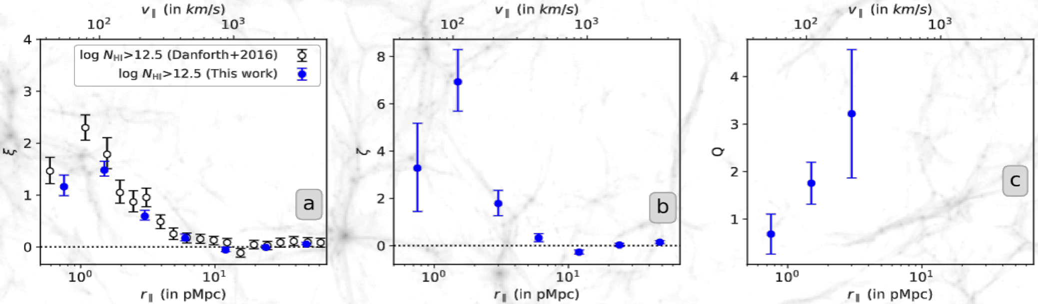

- 82 quasar sightlines from HST-COS
- Redshift based clustering study (colinear triplet configurations probed along quasar sightlines; $r_1 = r_2 = r_\parallel, r_3 = 2r_\parallel$).
- Lyman-α forest probed in $z < 0.48$.

Reduced ζ or Q=$\zeta/(\xi_1 \times \xi_2 + \xi_2 \times \xi_3 + \xi_3 \times \xi_1)$
[Hierarchical Ansatz]

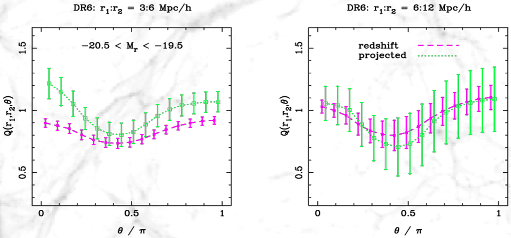

Clustering in SDSS galaxies: McBride+2010

First detection of non-gaussianity in low-z Lyman-α forest (Maitra+2020b)

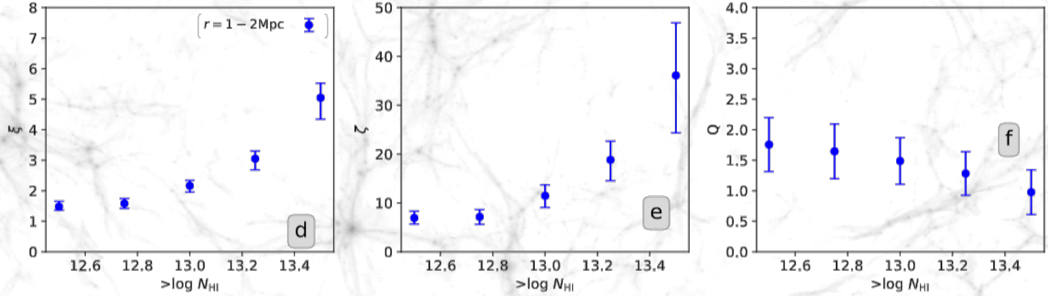

- HI column density($N_{\rm HI}$) $\Longleftrightarrow$ Baryonic overdensity (Δ).
- Strong dependence of ξ and ζ on $N_{\rm HI}$ thresholds.
- Effect on Q very weak.

First detection of non-gaussianity in low-z Lyman-α forest (Maitra+2020b)

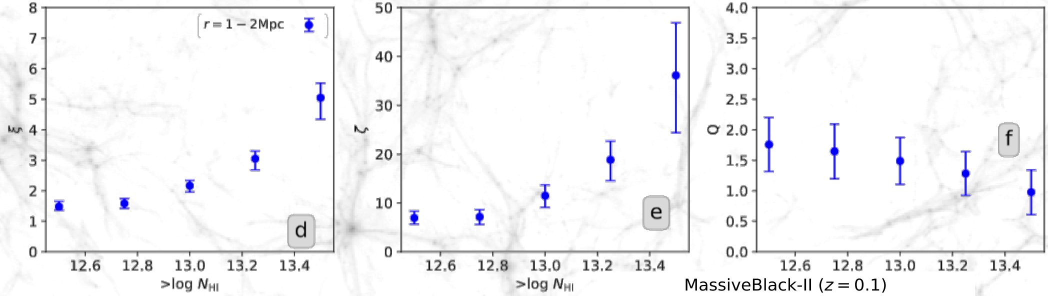

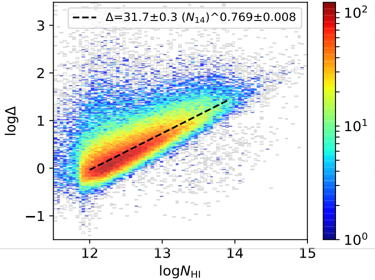

- HI column density($N_{\rm HI}$) $\Longleftrightarrow$ Baryonic overdensity (Δ).
- Strong dependence of ξ and ζ on $N_{\rm HI}$ thresholds.
- Effect on Q very weak.

First detection of non-gaussianity in low-z Lyman-α forest (Maitra+2020b)

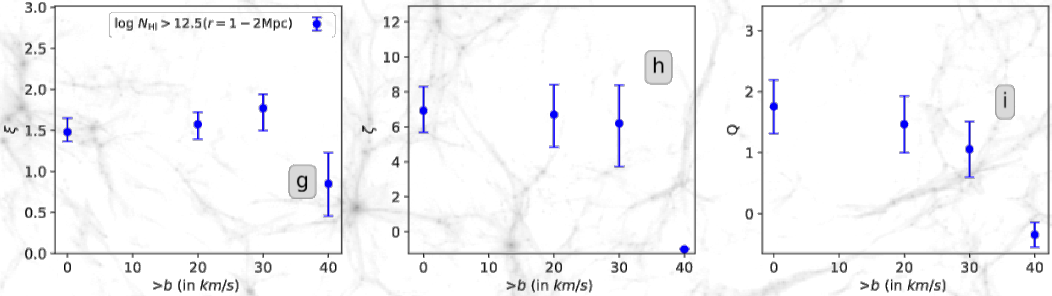

- Weak dependence on line-width parameter $b = \sqrt{2kT/m}$ upto a b threshold of $30 km/s$. Sharp decrease in correlation amplitude at $b > 40 km/s$ (Broad Lyman-α Absorbers or BLAs).
- Frequency of occurrence of atleast 1 BLAS in triplet systems ($\sim$88%) is a factor ~ 3 higher than that found among the full sample ($\sim$32%).
- BLAs possibly trace the warm-hot intergalactic medium (WHIM) in the temperature range between 10^5 and 10^6 K (Richter+2006). Arises from collisionally ionized regions in filaments.

First detection of non-gaussianity in low-z Lyman-α forest (Maitra+2020b)

Association with metal systems and galaxies:

- Only 40% of the total observed Lyman-α triplets have associated metals with them.
- Majority of the triplets have multiple nearby galaxies.
- 84% of the triplets have at least one nearby galaxy within a velocity separation of $500 km/s$. The impact parameters of these galaxies range from 62-3854 pkpc (median of 405 pkpc)
- The median impact parameter seems to decrease for higher N_{HI} thresholds.
- BLAs occuring more frequently with triplets and association with nearby galaxies suggest Lyman-α triplets originating from filamentary structures.

Trends in simulations:

- Simulations suggest line of sight peculiar velocities tend to enhance the observed ξ and ζ by $\sim$60%, whereas the Q values are suppressed by $\sim$70%.
- Feedback processes have little effect on the observed clustering.

Detection of non-gaussianity in high-z Lyman-α forest (In prep.)

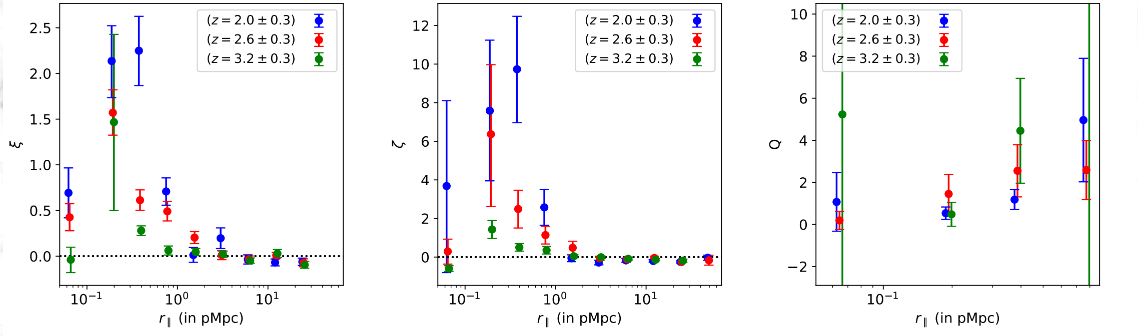

Figure: High-z correlations of $N_{\rm HI} > 10^{13.5}{\rm cm}^{-2}$ in KODIAQ data.

Work in progress ...

Transverse three-point correlation in Simulations at $z \sim 2$ (Maitra+2020a)

- Δ, v,T obtained from GADGET-3 hydrodynamical simulation.
- Shoot triplet sightlines through simulation box.
- Investigate ζ and its dependencies on:
  - Scale.
  - Angle.
  - N_{HI} or conversely Δ.
  - Thermal history.
- We consider only isosceles configurations for ζ ($\Delta r_{12\perp} = \Delta r_{13\perp} = r$).

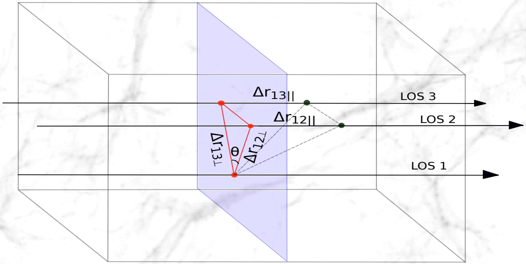

Transverse three-point correlation in Simulations at $z \sim 2$ (Maitra+2020a)

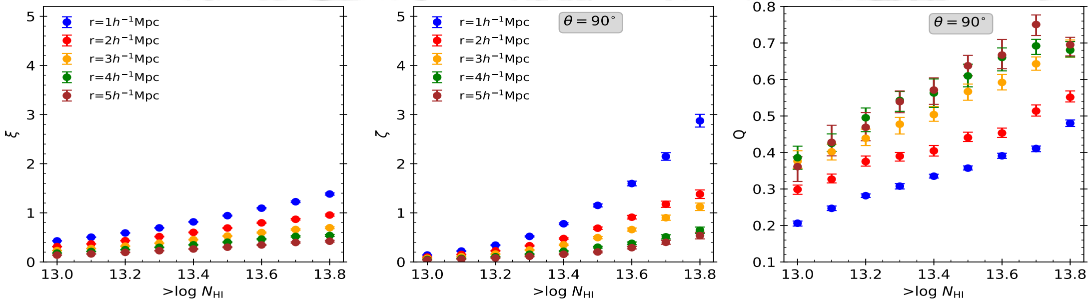

Transverse three-point correlation in Simulations at $z \sim 2$ (Maitra+2020a)

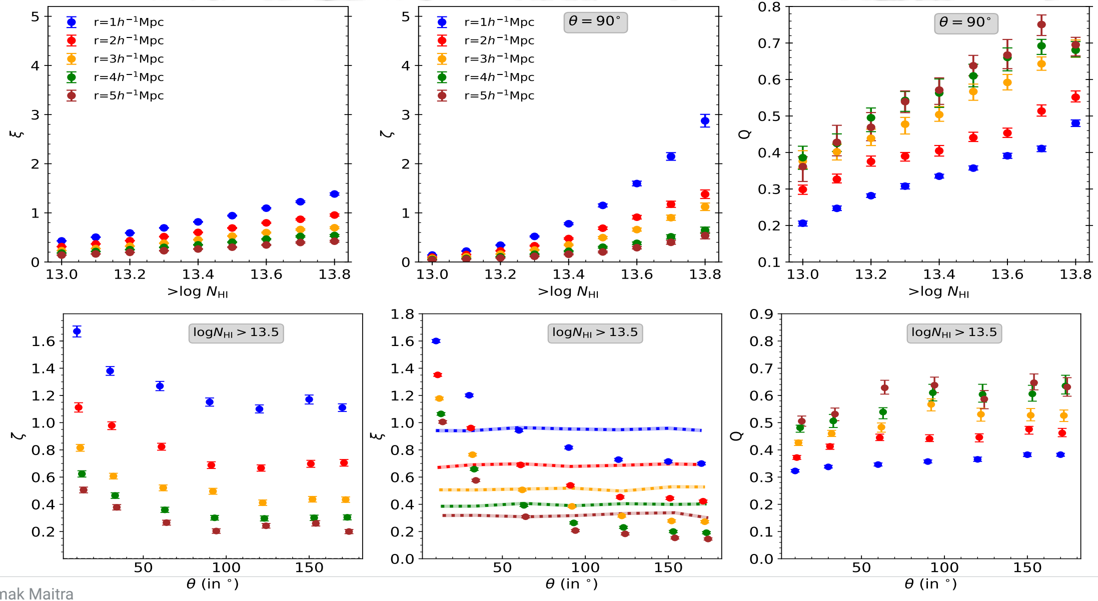

Transverse three-point correlation in Simulations at $z \sim 2$ (Maitra+2020a)

Effect of thermal history:

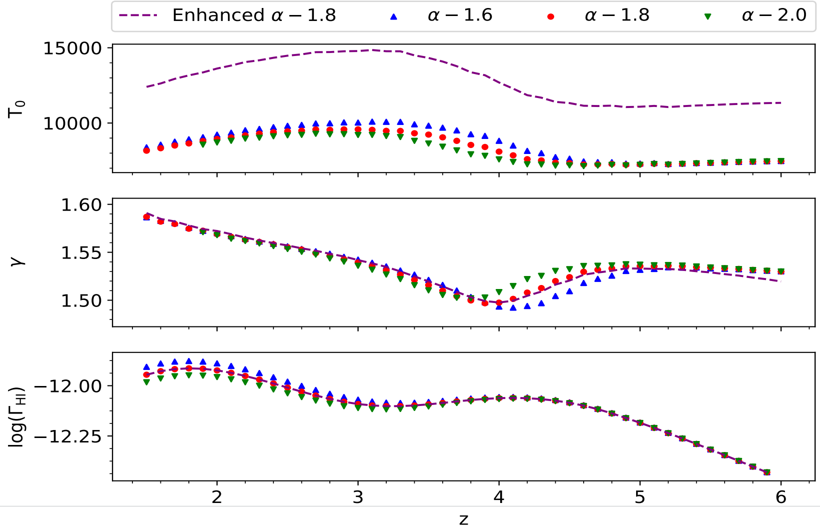

Transverse three-point correlation in Simulations at $z \sim 2$ (Maitra+2020a)

Effect of thermal history:

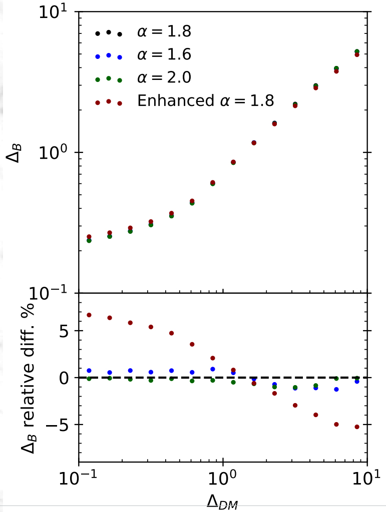

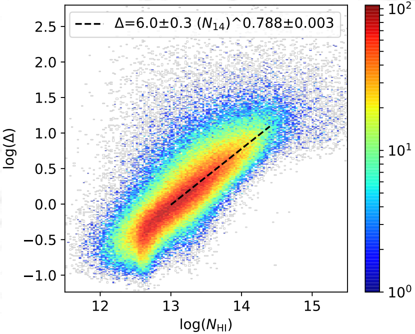

- Correlations for a fixed $N_{\rm HI}$ threshold depends on Δ field + local thermal effects.
- Local thermal effects are imprinted on the Δ to $N_{\rm HI}$ mapping.
- Using a constant Δ threshold should statistically show the effects of pressure broadening.

Transverse three-point correlation in Simulations at $z \sim 2$ (Maitra+2020a)

Effect of thermal history:

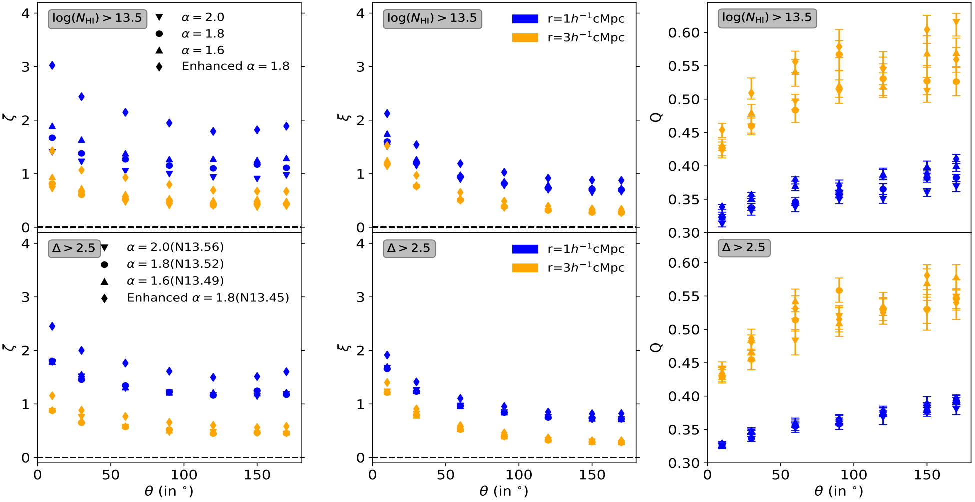

Validity of Hierarchical Ansatz:

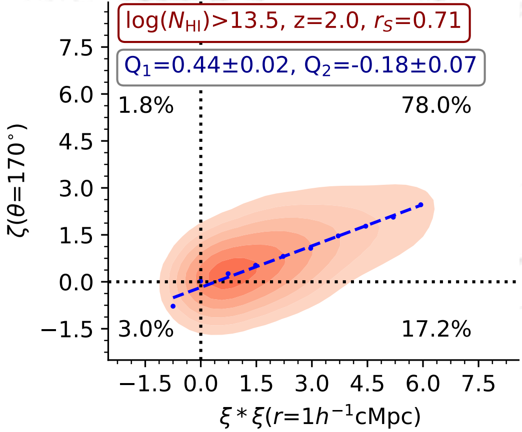

$$\zeta = Q_1(\xi * \xi) + Q_2$$

Transverse three-point correlation in Simulations at $z \sim 2$ (Maitra+2020a)

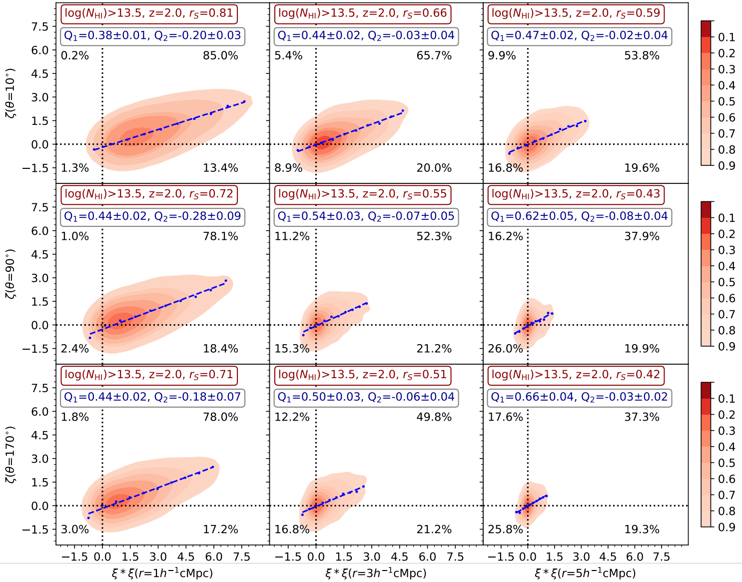

Transverse three-point correlation in Simulations at $z \sim 2$ (Maitra+2020a)

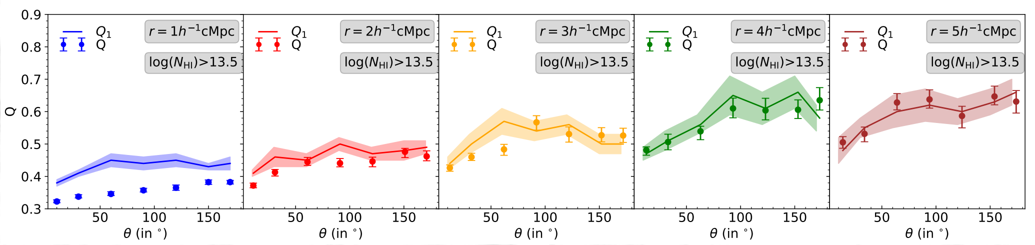

Three-point correlation suppressed at scales below $3h^{-1}$cMpc [Q_2 -ve]. Source?

Transverse three-point correlation in Simulations at $z \sim 2$ (Maitra+2020a)

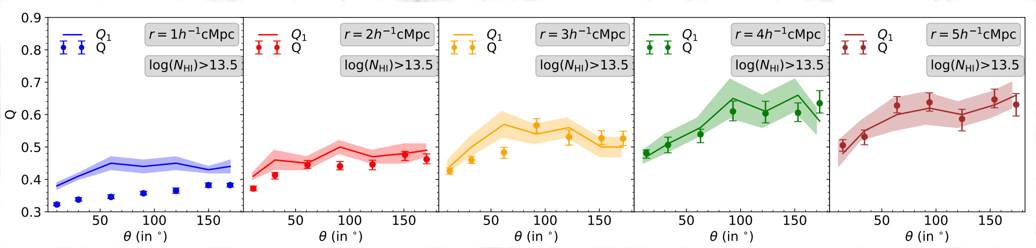

Three-point correlation suppressed at scales below $3h^{-1}$cMpc [Q_2 -ve]. Source?

We used the SDSS catalog to get an estimate of the number of quasar triplets present and achievable significance of three-point correlation detection with these sample of quasars.

- For $\theta \leq 20^\circ$, ζ can be observed the scales of 4 and $5h^{-1}$cMpc with 4.8σ and 4.5σ respectively. For that, we need to observe 70 quasar triplets (210 spectra) having $r = 4h^{-1}$cMpc and 86 quasar triplets (i.e 258 spectra) having $r = 5h^{-1}$cMpc.
- For $\theta = 90^\circ$, the most significant detection can be achieved for 2 and $3h^{-1}$cMpc (4.4σ and 4.7σ respectively). We need to observe 42 quasar triplets having $r = 2h^{-1}$cMpc and 96 quasar triplets having $r = 3h^{-1}$cMpc.

Observational prospects with QSO triplet sightlines (Maitra+2019)

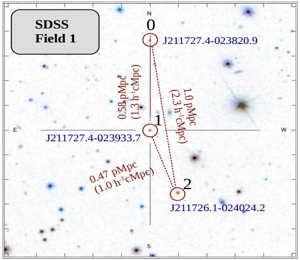

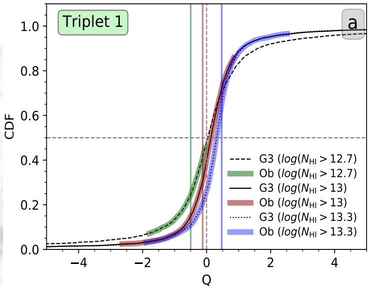

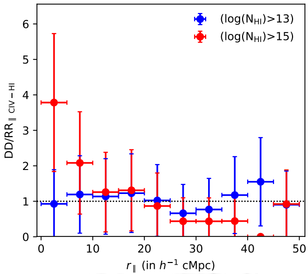

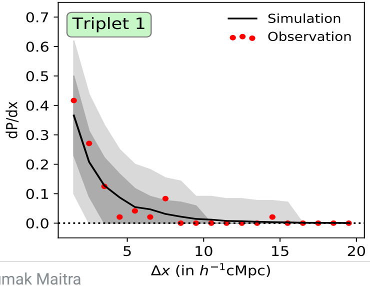

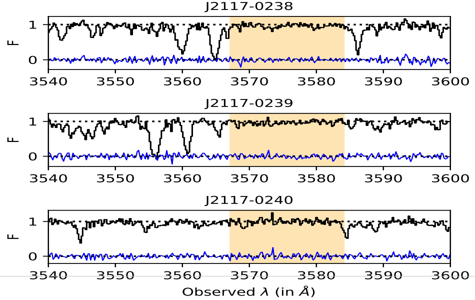

Future plan

- Extend study to non-standard ΛCDM models.
- We would like identify filamentary structures associated with galaxies (near observed Lyman-α triplets) and try to explore the association of such structures with observed Lyman-α triplets.
- Investigate partial redshift space + transverse three-point correlation using projected quasar pairs (Findlay+2018).
- We identified a unique configuration of 7 quasars (with $r < 20.5$ and $z > 2.2$) in SDSS catalog that opens the opportunity to probe correlated IGM structures at $z \sim 2$. Use these 7 quasar sightlines to study the directional dependence of density/radiation field around the foreground QSOs through the analysis of the transverse proximity effect.
- Theoretical understanding of metal distribution in IGM (project led by Sukanya Mallik, IUCAA).
- Inversion problem: Mapping the observed transmitted flux to underlying overdensity and velocity fields.